THE UNIVERSITY of EDINBURGH

Edinburgh Research Explorer

Progressive Neuronal Pathology and Synaptic Loss Induced by Prediabetes and Type 2 Diabetes in a Mouse Model of Alzheimer's Disease

Citation for published version:
Ramos-Rodriguez, JJ, Spires-Jones, T, Pooler, AM, Lechuga-Sancho, AM, Bacskai, BJ & Garcia-Alloza, M 2016, 'Progressive Neuronal Pathology and Synaptic Loss Induced by Prediabetes and Type 2 Diabetes in a Mouse Model of Alzheimer's Disease', *Molecular Neurobiology*, vol. 53. https://doi.org/10.1007/s12035-016-9921-3

Digital Object Identifier (DOI):
10.1007/s12035-016-9921-3

Link:
Link to publication record in Edinburgh Research Explorer

Document Version:
Peer reviewed version

Published In:
Molecular Neurobiology

General rights
Copyright for the publications made accessible via the Edinburgh Research Explorer is retained by the author(s) and / or other copyright owners and it is a condition of accessing these publications that users recognise and abide by the legal requirements associated with these rights.

Take down policy
The University of Edinburgh has made every reasonable effort to ensure that Edinburgh Research Explorer content complies with UK legislation. If you believe that the public display of this file breaches copyright please contact openaccess@ed.ac.uk providing details, and we will remove access to the work immediately and investigate your claim.

Download date: 23. Jul. 2021

Manuscript
Click here to download Manuscript Paper Pre-T2D-AD-Neur 6. Mol Neurobiol.doc

Progressive neuronal pathology and synaptic loss induced by prediabetes and type 2 diabetes in a mouse model of Alzheimer's disease

Juan Jose Ramos-Rodriguez (1), Tara Spires-Jones (2), Amy M. Pooler (2, 3), Alfonso Maria Lechuga-Sancho (4), Brian J. Bacskai (2), Monica Garcia-Alloza (1)

(1) Division of Physiology. Institute of Biomolecules (INBIO). School of Medicine. Universidad de Cadiz (Spain).

(2) Department of Neurology. MGH. Harvard Medical School, Charlestown (USA).

(3) Institute of Psychiatry, Psychology & Neuroscience, Dept of Basic and Clinical Neuroscience, King's College London, London (UK)

(4) Department of Pediatrics, School of Medicine. University of Cadiz (Spain).

Corresponding author:

Monica Garcia-Alloza, PhD

Division of Physiology, School of Medicine

University of Cadiz

Plaza Fragela 9, 4 piso, 410

Cadiz (11003)

Tel: +34 956015252

Email: monica.garcia@uca.es

Abstract

Age remains the main risk factor for developing Alzheimer's disease (AD) although certain metabolic alterations, including prediabetes and type 2 diabetes (T2D), may also increase this risk. In order to understand this relationship, we have studied an AD-prediabetes mouse model (APP/PS1) with severe hyperinsulinemia induced by long-term high fat diet (HFD), and an AD-T2D model, generated by crossing APP/PS1 and db/db mice (APP/PS1xdb/db). In both, prediabetic and diabetic AD mice, we have studied underlying neuronal pathology and synaptic loss. At 26 weeks of age, when both pathologies were clearly established, we observed severe brain atrophy in APP/PS1xdb/db animals as well as cortical thinning, accompanied by increased caspase activity. Reduced senile plaque burden and elevated soluble Aβ40 and 42 levels were observed in AD-T2D mice. Further assessment revealed a significant increase of neurite curvature in prediabetic-AD mice, and this effect was worsened in AD-T2D animals. Synaptic density loss, analyzed by array tomography, revealed a synergistic effect between T2D and AD, whereas an intermediate state was observed once more in prediabetic-AD mice. Altogether, our data suggest that early prediabetic hyperinsulinemia may exacerbate AD pathology, and that fully established T2D clearly worsens these effects. Therefore it is feasible that early detection of prediabetic state and strict metabolic control could slow or delay progression of AD-associated neuropathological features.

Key words: hyperinsulinemia, type 2 diabetes, Alzheimer’s disease, array tomography, axonal curvature, synaptic density.

Background

Alzheimer's disease (AD) is the most common cause of dementia among elderly people and at present it has no successful treatment. Neuropathological features include senile plaques (SP), mainly composed of amyloid-β (Aβ), and neurofibrillary tangles, comprised of phosphorylated tau [1]. More than these classical lesions, synaptic loss and reduced expression of synaptic proteins are the strongest pathological correlate of dementia and have the potential to may be more reliable markers of the progression of AD [2-3].

Although age remains the main risk factor for AD, the ultimate causes are not completely understood. Epidemiological, clinical and animal studies also support that prediabetes [4-6] and type 2 diabetes (T2D) [7-9] may also be influential risk factors to develop AD and since prediabetes, although still reversible, goes largely undiagnosed in the population, it might be a critical control point. Previous studies have described links between T2D and AD which associate both pathologies. Among others, insulin receptors in the central nervous system are highly expressed in cognition-related regions, such as cortex and hippocampus, consistent with evidence showing that insulin levels influence memory [10]. Aβ oligomers, likely the most toxic Aβ species, may directly interfere with insulin signalling in hippocampal neurons resulting in memory dysfunction [11]. Aβ accumulation is currently seen as a key step in the pathogenesis of AD [12] and insulin may regulate Aβ levels [13-14], as well as exacerbate inflammatory responses that promote pathological Aβ processing and deposition (for review see [15-17]). Furthermore, reduced brain insulin signalling in mouse models of diabetes increases tau phosphorylation and Aβ levels [18-19]. Nevertheless, the mechanisms underlying the relationship between diabetes and dementia have not been completely elucidated.

Recently, various transgenic animal models have been developed in order to further explore this relationship and derived consequences, including prediabetic and diabetic AD models [20-21]. In the present study we have used two animal models: 1) a prediabetic hyperinsulinemic AD mouse line, induced by long-term high fat diet (HFD) administration to APPswe/PS1dE9 mice (APP/PS1) [20], and 2) a long-term type 2 diabetic AD mouse, by using a mixed model of AD

(APP/PS1 mouse) and a T2D (db/db mouse) (APP/PS1xdb/db) [19]. These mouse lines allowed us to study the specific role of both, prediabetes and T2D, in the development of AD pathology, including generation of Aβ species or brain atrophy, as well as specific neuronal alterations such as axonal curvature and synaptic loss. Together, our data suggest that early hyperinsulinemia is sufficient to exacerbate central pathology in APP/PS1 mice, and that this effect further worsens when T2D diabetes is completely established.

Methods

1. Animals

APPswe/PS1dE9 mice were obtained from the Jackson Laboratory (Bar Harbor, USA) [22-23]. Prediabetes was induced in wildtype and APP/PS1 mice as previously described [24] by feeding them with high-fat diet (HFD; 60% Kcal from fat, OpenSource, USA) from 4 weeks of age until sacrifice at 26-27 weeks of age. Wildtype and APP/PS1 mice received regular diet (RD) (SAFE A04. Augy, France).

In order to compare the effects of prediabetes and diabetes on brain pathology, APP/PS1 mice were crossed with db/db mice (Harlan Laboratories, The Netherlands) [19]. In order to characterize the effect of type 2 diabetes on AD pathology, 26-27 weeks old animals were grouped as follows: control (APP/PS1$^{-/-}$db/db$^{+/+}$, APP/PS1$^{-/-}$db/db$^{+/-}$ mice), APP/PS1 (APP/PS1$^{+/-}$db/db$^{+/+}$ and APP/PS1$^{+/-}$db/db$^{+/-}$ mice), db/db mice (APP/PS1$^{-/-}$db/db$^{-/-}$) and APP/PS1xdb/db (APP/PS1$^{+/-}$db/db$^{-/-}$ mice), since db/db mice only show diabetic phenotype when homozygous for the leptin receptor knockout (db/db$^{-/-}$). In order to compare groups all mice were sacrificed at 26-27 weeks of age, when induced prediabetes or T2D are completely established and AD related pathology has also commenced in APP/PS1 mice.

All experimental procedures were approved by the Animal Care and Use Committee of the University of Cadiz, in accordance with the Guidelines for Care and Use of experimental animals (European Commission Directive 2010/63/UE and Spanish Royal Decree 53/2013).

2. Metabolic determinations

Body weight, postprandial blood glucose and plasma insulin levels were determined immediately before sacrifice in all groups, as previously described [24]. Blood glucose levels were measured from nicked tails using the glucometer Optium Xceed (Abbott, United Kingdom). Plasma insulin levels were measured using ultrasensitive mouse enzyme-linked immunoabsorbent assay (ALPCO Diagnostics, Salem, NH).

3. Tissue processing

At 26-27 weeks of age, animals were overdosed with chloral hydrate (60 mg/Kg). Brains were harvested and immediately weighed. Cortical tissue was dissected from the right hemisphere and stored at -80ºC prior to use. A small portion of the sensorimotor cortex (~1mm^3) was also dissected for array tomography studies and fixed as previously described [25]. Left hemispheres were fixed in 4% PFA for two weeks before 30 µm coronal brain sections were obtained using a Microm HM450 microtome (ThermoFisher, Spain) and stored in 50% polyethyleneglycol at 4ºC.

4. Cresyl violet staining

Sections were selected at 1.5, 0.5, -0.5, -1.5, -2.5 and -3.5 mm from Bregma [26], as previously described [24], in order to analyze the cortex from all mice groups. Sections were mounted with DPX (Sigma, St. Louis, MO, USA) and images were acquired using an optical Laser Olympus U-RFL-T microscope (Olympus, Japan) and MMIcellTools software. Cortical thickness was measured in frontal, parietal and temporal cortical sections using Adobe Photoshop Elements and Image J software.

5. Caspase activation

Caspases 3/7 activity was analyzed in cortical homogenates from all groups in this study using the Caspase-Glo 3/7 assay (Promega, Madrid, Spain), following manufacturer´s indications.

Briefly, 5-7 mg of cortex was homogenized in PBS supplemented with a protease cocktail (Sigma, USA). Samples were diluted with PBS (2 µg/µl) and 50 µl of tissue homogenate was added to 50 µl of Promega Caspase-Glo 3/7 assay solution. Samples were incubated 1 hour at room temperature, protected from light. Luminescence signal was measured in the Biotek Synergy Mx Microplate Reader and data were expressed as percentage of control values.

6. Senile plaque quantification

Cortical Aβ burden was quantified in consecutive sections to those used for cresyl violet staining as previously described [27]. Sections were incubated with anti-Aβ antibody 1:2000 (AB2287 Millipore, USA) in 0,5% BSA overnight at 4ºC. Secondary antibody, donkey anti-rabbit Alexa Fluor 594 (Molecular Probes, OR, USA) 1:1000, in 0.5% BSA, was incubated for 1 h at room temperature. Tissue was incubated with thioflavin-S (TS) 0,005% (Sigma, USA) 10 min at room temperature for dense core SP. Sections were visualized with a laser Olympus U-RFL-T fluorescent microscope (Olympus, Japan). Images were acquired using MMIcellTools software and analyzed with Image J software to quantify Aβ and TS burdens.

7. Aβ40 and Aβ42 levels

Soluble and insoluble Aβ40 and 42 concentrations were measured in cortical homogenates using colorimetric ELISA kits (Wako, Japan, Aβ 40 ref: 294-62501 and Aβ 42 ref: 290-62601) as previously described [28]. Assay was run following manufacturer's indications and read at 450nm. Data were expressed as ng/mg tissue.

8. NeuN and DAPI staining

PFA-fixed 30 µm sections were washed in PBS, pretreated with 70% formic acid for 10 min and subsequently blocked in 5% normal goat serum (NGS) and 0,5% Triton-X100 for 1h. Sections were immunostained with anti-NeuN antibody (Chemicon) 1:200 as previously described [29], and conjugated goat anti-mouse Alexa Fluor 594 was used as secondary antibody. Sections

were washed and stained with DAPI 1mg/ml (Sigma) (1:2000) to stain nuclei and TS (0.005%) to visualize SP. The percentage of NeuN-possitive cells (normalized by total cells stained with DAPI was quantified in the proximity of SP in APP/PS1, APP/PS1-HFD and APP/PS1xdb/db mice (up to 40 μm). Areas located far from SP were also compared with Control, Control-HFD and db/db mice using Image J software.

9. Axonal inmunostaining

Axonal curvature was determined by immunostaining with SMI-312R antibody (1:1000) (Covance, USA) on consecutive sections to those used for cresyl violet staining. Briefly, sections were pretreated with hydrogen peroxide 3% and Triton-X 0.5% 20 min at room temperature and blocked with 3% BSA 1 hour. Alexa Fluor goat anti-mouse 594 was used as secondary antibody (Molecular Probes, USA) 1:200, in 1% NGS for 1h at room temperature. Senile plaques (SP) were visualized by staining with TS (0.005% w/v). Micrographs of stained tissue were obtained with a Laser Olympus U-RFL-T fluorescent microscope (Olympus, Japan) and MMIcellTools software. Axon curvature ratio was calculated by dividing the end-to-end distance of a dendrite segment by the total length between the two segment ends. Axon distance to the closest SP was measured at three points along each dendrite and the average distance was taken from these three measurements [30]. Axon curvature ratio and distance to SP were measured using Image J software. Curvatures were pooled in 10 μm steps from SP up to 40 μm from the border, and neurites analyzed further from SP borders were considered in SP-free areas. In SP-free animals axon curvature was compared with those measured in APP/PS1 mice further than 40 μm from SP.

10. Array tomography

Array tomography in combination with immunohistochemistry is a powerful approach to assess synaptic density in small tissue blocks. Synaptic density was assessed in 26-27 week old mice. Tissue from all groups under study was prepared for array tomography as previously described [25]. Briefly, cortical samples were fixed in 4% PFA for 4 hours, dehydrated through increasing

serial dilutions of ethanol and immersed into LR White resin (Electron Microscopy Sciences) to polymerize overnight at 53 °C. Embedded blocks were cut into ribbons (70 nm) by ultracut microtome (Leica) using a Jumbo Histo Diamond Knife (Diatome). Sections were rehydrated for 5 min with 50 mM glycine in TBS and blocked 5 min in 0.05% Tween and 0.1% BSA. Primary antibodies for PSD95 (Abcam, USA) and 6E10 for Aβ (Covance, USA) were incubated (1:50) in blocking buffer overnight at 4ºC. Secondary antibodies (Jackson ImmunoResearch, USA) were incubated at 1:50 in blocking buffer for 30 minutes. Sections were counterstained with 0.01 mg/mL DAPI for 20 min. For each area of interest (identified by fiduciary markers, such as nuclei), images were obtained on 18–25 serial sections through the somatosensory cortex using a Zeiss AxioImager Z2 microscope (Zeiss, Germany). Each set of images were opened sequentially in Image J, aligned, and processed in Watershed software (courtesy of Brad Busse and Steven Smith) to detect puncta larger than 10 voxels in volume that were present in more than one consecutive section. Synapse densities were calculated by dividing the number of PSD95-positive puncta by the volume of tissue sampled. The combined role of SP "halo effect" and metabolic alterations on synaptic density was assessed up to 40 µm from plaque borders (in 10 µm steps) in SP-bearing groups. The number of PSD95 dots in SP-free mice was compared with APP/PS1 mice densities when distance from SP were >40 µm.

11. Statistical analysis

Control groups from prediabetic (wildtype-RD) and T2D (APP/PS1$^{+/+}$db/db$^{+/+}$ and APP/PS1$^{+/+}$db/db$^{+/-}$) studies were compared and no differences were observed. Therefore all animals were included as a single control group. Two-way ANOVA (groupXdistance from SP) was used to compare synaptic density and axonal curvature. Further analyses by one-way ANOVA for independent samples were performed for individual distance subsets studied. One-way ANOVA was used to compare metabolic parameters, Aβ levels, caspase activation and cortical thickness. Correlation studies were performed using Pearson´s correlation test.

Results

1. Metabolic characterization

Body weight was significantly increased in both control and APP/PS1 mice on HFD for 23 weeks (table 1), and this effect was higher T2D mice, both db/db and APP/PS1xdb/db. Although a slight increase in glucose levels was observed in APP/PS1-HFD treated mice, differences did not reach statistical significance, and were below 300 mg/dl, as a control limit for diabetes [24]. Conversely, T2D mice showed a significant increase in glucose levels, clearly over 300 mg/dl, when db/db and APP/PS1xdb/db mice were compared (table 1). Plasmatic insulin was significantly increased in control-HFD mice and even higher values were detected in APP/PS1-HFD mice (table 1), supporting long-term HFD as a model of hyperinsulinemia and prediabetes [24]. When we analyzed diabetic mice we also observed a significant increase in insulin levels in db/db and a slightly higher, non significant increase was also detected in APP/PS1xdb/db mice (table 1).

2. T2D induced atrophy is worsened in AD-T2D mixed model

A slight, non significant, reduction in brain weight was observed in APP/PS1-HFD mice. As previously reported, a significant reduction of brain weight was observed in db/db mice [24]. Brain weight reduction was maximal in APP/PS1xdb/db mice, suggesting a step-wise worsening effect from prediabetes to diabetes, and supporting a synergistic interaction between the presence of APP/PS1 transgenes and db/db induced metabolic alterations [20] (Figure 1A). In accordance with macroscopic observations, we detected a reduction of cortical thickness in db/db mice [31], that was further exacerbated in APP/PS1xdb/db mice (Figures 1B and 1C).

3. Caspase activation and neuronal loss is progressively increased in AD-prediabetic and diabetic mice

Caspases 3/7 activation were similar to controls in the cortex from APP/PS1 and APP/PS1-HFD mice. However, we detected a significant increase in activation of cortical caspases 3/7 in db/db mice. This effect was further increased in APP/PS1xdb/db mice (Figure 2A). The specific effect

of the atrophy and cell death, on neurons was also assessed. In SP-free areas, the percentage NeuN-positive cells was slightly reduced in APP/PS1-HFD mice, and this effect was worsened in db/db mice. Moreover, in APPP/PS1xdb/db mice neuronal loss was increased when compared with the rest of the groups (Figures 2B and 2C). In the close proximity of SP a relevant reduction in the NeuN+/DAPI ratio was detected in all groups (APP/PS1, APP/PS1-HFD and APP/PS1xdbdb) when compared with SP free areas, however even higher reductions were observed in the mixed model, APP/PS1xdb/db also in the proximity of the plaques (Figures 2B and 2C).

4. Altered Aβ pathology in prediabetic and diabetic APP/PS1 mice

As previously shown, prediabetes and diabetes do not necessarily affect amyloid pathology in the same manner [19-21, 32]. We observed an overall increase of SP in prediabetic APP/PS1 mice after long-term HFD, whereas a reduction in dense-core plaques stained with TS was observed in the mixed T2D-AD animal model (APP/PS1xdb/db) [19, 21] (Figures 3A and 3B). We corroborated these findings by measuring Aβ by ELISA and we detected increased insoluble Aβ40 levels in prediabetic APP/PS1 mice (Figure 3C). Treatment of APP/PS1 mice with HFD increased soluble Aβ40 and 42 levels, following a similar trend previously reported [20, 32], although differences only reached statistical significance in APP/PS1xdb/db mice, both for Aβ40 and 42 cortical levels (Figure 3C). As previously suggested, our data support a shift towards more toxic soluble species in our mixed APP/PS1xdb/db model.

5. Diabetes worsens AD neurite curvature

We analyzed neurite curvature as an indication of neuronal dysfunction, [33-35] in the proximity of SP bearing groups (APP/PS1, APP/PS1-HFD and APP/PS1xdb/db). We also compared neurite curvature in SP-free groups (control, control-HFD and db/db) and in SP-free areas from all APP/PS1 groups. Neurite curvature was not affected in control-HFD mice whereas a slight increase in neurite curvature was observed both in APP/PS1 and APP/PS1-HFD mice even in SP-free areas. This effect was more severe in db/db mice, suggesting that neuronal integration

is impaired in a T2D animal model. Furthermore, curvature ratios in SP-free areas were significantly worsened in APP/PS1xdb/db mice when compared to the rest of the groups, supporting a cross-talk between both pathologies (Figure 4A and 4B). Brain regions containing SP (APP/PS1, APP/PS1-HFD and APP/PS1xdb/db mice) presented increased curvature ratios, when compared to SP-free areas and mice without SP. This effect was worsened in animals harboring both T2D and AD (APP/PS1xdb/db) (Figures 4A and 4B). In plaque-bearing mice (APP/PS1, APP/PS1-HFD and APP/PS1xdb/db) we also analyzed the "halo" effect of SP on neurite curvature, by allocating measured neurons in 10 µm intervals from plaque border up to 40 µm. As expected, curvature ratio increased as distance to plaques was reduced and we detected a groupXdistance effect when we compared among groups [$F_{(8,4171)}$=1.967, *p=0.045]. Further analysis in different subsets revealed an intermediate increase of neurite curvature in APP/-PS1-HFD mice, that worsened in APP/PS1xdb/db mice (Figure 4C).

6. Amyloid-plaque induced synaptic loss is increased in diabetic mice

Synaptic density was reduced in APP/PS1 mice even far from SP. Interestingly, even in the absence of amyloid pathology, we also detected that db/db mice presented reduced synaptic densities, indicating that T2D alone can significantly impair synapses (Figures 5A and 5C). A significant reduction in synaptic density was detected in the close proximity of SP. This reduction was approximately 30% in APP/PS1 mice, compared to control mice, in the range of previous observations [25] and up to 50% reduction in APP/PS1xdb/db mice, supporting the synergistic effect between AD and T2D also on synaptic dysfunction (Figures 5A and 5C). Analysis also revealed a "halo" effect around SP, in agreement with previous work [25]. We did not detect a groupXdistance effect in synaptic density [$F_{(8,1027)}$=0.99, p=0.440], however further analysis of individual subsets revealed an overall exacerbation of synaptic loss in APP/PS1xdb/db mice (Figures 5B and 5C). Soluble Aβ40 and 42 levels negatively correlated with synaptic densities, reaching statistical significance far from SP (Pearson´s correlations: Aβ40-synaptic density (ρ=-0.664**) and β42 -synaptic density (ρ=-0.599**, **p<0.01). The fact that plaque-induced synaptic toxicity was increased in APP/PS1xdb/db mice, and that synaptic

density was still compromised far from SP (>40µm) in this group, supports a synergistic effect between amyloid pathology and metabolic alterations associated with T2D.

Discussion

Previous epidemiological and pre-clinical studies support a close relationship between AD and T2D (for review see [10, 17], however the underlying mechanisms are not completely understood. It also remains unclear whether hyperinsulinemia and insulin resistance, indicative of a prediabetic state prior to T2D, may also induce or accelerate central pathology in AD. Indeed, glucose and insulin play a crucial role in maintaining normal brain activity, and alterations of insulin dependent functions could be associated with central pathological conditions observed in AD [10, 15-16, 20, 24]. In order to address the role of T2D and prediabetes on neuronal and synaptic alterations in AD, we induced a severe hyperinsulinemia by long-term HFD administration to APP/PS1 mice. We also used a mixed animal model that presents both T2D and AD (APP/PS1xdb/db mouse) [19]. All animals under study were analyzed at 26-27 weeks of age, when SP deposition has commenced in APP/PS1 mice [23], and prediabetes, or diabetes has been completely established. Only T2D mice (db/db and APP/PS1xdb/db) presented glycaemia levels over 300 mg/dl, which is considered the threshold for a diagnosis of diabetes in rodents [20, 36]. HFD induced high insulin levels and this effect was worsened when diabetes was completely established. Prediabetic mice overweight increased in diabetic mice (both db/db and APP/PS1xdb/db). Altogether, metabolic parameters indicate a progressive worsening effect from prediabetes to completely established T2D.

Neuronal and synaptic loss are major hallmarks of AD, and brain atrophy is observed in both AD and T2D patients; however, one of the main limitations of present AD mouse models is that they show very little neuronal loss [37]. Diabetic (db/db) mice showed a significant reduction in brain weight, as previously described [24] and this effect was worsened in combination of APP/PS1 transgenes, suggesting that aggravated brain atrophy in APP/PS1xdb/db mice is due to a synergic effect between AD and T2D. Also, cortical grey matter was reduced in AD-T2D mice, which is in line with previous observations in T2D patients, who have diminished brain volume

and cortical grey matter [38-39]. Increased apoptosis in the APP/PS1xdb/db mice may be due to higher caspase activity. Indeed, we observed increases in caspase 3 and 7 in db/db mice, and even higher activity in APP/PS1xdb/db mice. Although caspase activation can not unequivocally determine cell apoptosis, it may contribute to synapse loss which ultimately casuses deafferntatiaion and cell death. [40]. Moreover NeuN/DAPI ratios were progressively reduced in prediabetic APP/PS mice, db/db and APP/PS1xdb/db mice, supporting a worsening prediabetes-to-diabetes effect. Reduced neuronal density might be due to increased gliosis, observed both in APP/PS1 and db/db animals [19]. However, our data in combination with previous studies, in which central proliferation and neurogenesis processes seem to slow with aging in db/db mice [31], might further underscore the mechanisms of the neurodegeneration which evolves in the mixed colony (APP/PS1xdb/db). Leptin signalling is involved in synaptic function, neurodegeneration or learning and memory formation [41-42], and therefor our observations might not exclusively due to diabetes. However, our AD-prone prediabetic model (APP/PS1-HFD) showed a small reduction in brain weight, cortical thickness and neuronal population, suggesting the possibility of an intermediate state, before T2D onset, that could reveal some early prediabetes-related loss of neuronal integrity.

Whereas peripheral neuropathy has been widely addressed in T2D, central neuronal pathology associated is not so well characterized. It has been previously stated that, just as any other insulin-dependent metabolically active tissue, neurons also develop insulin resistance and can not respond to insulin, resulting in neuronal injury (for review see [43]). In order to further characterize the observed brain atrophy in our mixed model of T2D and AD, we examined neurite curvature, as an indicator of abnormal neuronal morphology correlated with neuronal dysfunction (Stern et al. 2004). In AD mice, SP plaques can distort neurites in the close proximity and a "halo" effect of neurite pathology is clearly observed surrounding the plaques [35]. Whereas this effect has been largely addressed in AD models, to our knowledge no previous assessment of central axon curvature has been performed in db/db mice.We observed that even in the absence of plaques, T2D in db/db mice is sufficient to distort neuronal curvature, suggesting that synaptic transmission is also dysfunctional [44]. As expected, the presence of plaques in APP/PS1 mice caused an increase of axonal curvature, that was

worsened in the proximity of the plaques. Comparison of SP-bearing transgenic mouse groups showed that prediabetic mice (APP/PS1-HFD) had a more robust "halo" effect on abnormal curvature which again suggests an intermediate state in case of prediabetic mice. Abnormal neurite curvature was further exacerbated in APP/PS1xdb/db mice. Since T2D is a metabolic disorder that also provokes micro and macrovascular complications, inflammation and increased oxidative stress [17], several mechanisms may be responsible for increased neuritic curvature in the combined T2D-AD mouse line (APP/PS1xdb/db), as previously observed in other AD models [30, 34-35]. While we did not perform behavioural studies, it has been previously shown that both prediabetes and diabetes-induced states in APP/PS1 mice significantly impair learning and memory abilities [19-20]. Moreover, metabolic alterations significantly correlate with central pathology in both models, supporting the role of metabolic alterations at central level.

We also analyzed synaptic density by array tomography, allowing the study a great amount of synapses [25], represented by PSD95-positive synaptic puncta. We observed a similar profile to that detected for neurite curvature, with db/db mice displaying significant reduction of synaptic density, supporting the neurotoxic effect of T2D on the brain. Extensive evidence shows that Aβ in different states of aggregation, ranging from soluble species to dense core plaques, are neurotoxic [25, 35, 45]. Prediabetic AD mice presented an intermediate state, displaying some synaptic loss. However, the largest reduction in synaptic density was observed in APP/PS1xdb/db mice and synapse loss is the strongest correlate of cognitive decline in AD [1]. It has been previously shown that the space occupied by SP dense core, results in almost a total loss of synapses [25] and we also observed that the striking reduction in PSD95-positive puncta in the close proximity of the plaques, which has been shown to coincide with a "halo" of oligomeric Aβ surrounding the plaques [25], was worsened in APP/PS1xdb/db mice. This observations are also in agreement with detected soluble Aβ levels: increased soluble Aβ40 and 42 levels were detected in APP/PS1-HFD mice, which were even higher in APP/PS1xdb/db mice [19-21]. On the other hand SP burden was reduced in APP/PS1xdb/db mice, as previously described in this animal model [19, 46]. We can not exclude that Aβ might be preferentially

depositing as amyloid angiopathy in leptomeningeal vessels, instead of SP, in APP/PS1 mice. Our data might be in accordance with recent hypothesis on amyloid-dependent and amyloid-independent stages of AD, with an initial phase mediated by soluble oligomeric and fibrilar Aβ accumulation that leads to disruption of the neuropil, loss of dendritic spines, remodeling of neurites, and inflammatory responses, followed by a second phase that would consist of the further development of tangles, and synaptic and neuronal loss [12]. It is feasible that the observed increase in toxic soluble species [47] might contribute to progressive synapse reduction in prediabetic and diabetic AD mice. The combination of AD with T2D may therefore shift Aβ pathology towards a more severe version of the disease, which ultimately contributes to abnormal axonal curvature and synaptic loss.

Our data support a synergy between T2D and AD [19-20]. AD brain pathology was initially exacerbated in prediabetes and significantly worsened after diabetes was fully established. These data support the potential use of insulin resistance therapies and a tight metabolic control in diabetic patients, to prevent or delay associated central complications, including AD. Interestingly, our data on prediabetes suggests that, since this is still a reversible metabolic state, brain associated alterations could also be potentially reversible with good metabolic control, stressing the relevance of an early detection and management of insulin resistance.

Acknowledgements

Junta de Andalucia, Proyectos de Excelencia, Consejería de Economía, Innovación, Ciencia y Empleo (P11-CTS-7847), Fundación Eugenio Rodríguez Pascual 2015, ISCIII–Subdirección General de Evaluación y Fomento de la Investigación and cofinanced by the European Union (Fondo Europeo de Desarrollo Regional, FEDER) "Una manera de hacer Europa" PI12/00675 (Monica Garcia-Alloza).

Table 1. Effect of prediabetes and T2D on metabolic parameters in APP/PS1 mice

	Body weight (g)	Glucose (mg/dl)	Insulin (ng/ml)
Control	32.26±2.90	124.23± 4.80	0.93±0.174
Control-HFD	39.75±2.29††	129.63±11.29	6.52±1.69††
APP/PS1	30.51±1.05	125.04± 4.66	0.77±0.15
APP/PS1-HFD	41.13±2.84††	148.18± 9.88	8.45±2.31††
db/db	58.40±1.10**	455.67±43.72**	16.58±5.00**
APP/PS1xdb/db	57.37±2.74**	445.73±41.59**	20.65±6.91**

Metabolic parameters were determined in prediabetic mice (APP/PS1 and Control mice on HFD) as well as in diabetic mice (db/db and APP/PS1xdb/db). Data are representative of 8-31 mice and differences were detected by one-way ANOVA followed by Tukey b test or Tamhane tests as required. Body weight was significantly increased in HFD treated mice and higher increases were observed in T2D mice [$F_{(5,90)}$=64.36, **p<0.01 vs. rest of the groups, ††p<0.01 vs. control and APP/PS1 groups]. Glucose levels were slightly increased in APP/PS1 mice on HFD, although differences did not reach statistical significance. Glucose levels were significantly increased in T2D mice, both db/db and APP/PS1xdb/db [$F_{(5,90)}$=66.52, **p<0.01 vs. rest of the groups]. Insulin levels were increased in HFD treated mice and higher levels were detected in T2D mice. Although statistical differences were not detected, hyperinsulinemia was more severe in APP/PS1xdb/db mice [$F_{(5,45)}$=9.5, **p<0.01 vs. rest of the groups, ††p<0.01 vs. Control and APP/PS1 groups].

Figure 1. Cortical atrophy in APP/PS1-HFD mice is worsened in APP/PS1xdb/db mice. A) Brain weight was compared in all groups under study. A slight reduction in brain weight was observed in APP/PS1-HFD mice. Further atrophy was observed in db/db mice and this effect was worsened in APP/PS1xdb/db mice [$F_{(5,91)}$=37.5, **p<0.01 vs. rest of the groups, ††p<0.01 vs. APP/PS1-HFD, control-HFD, APP/PS1 and control mice, ‡‡p<0.01 vs. control and APP/PS1 mice]. **B)** Cortical thickness was reduced in db/db mice and further reduced in APP/PS1xdb/db mice. 1.5 mm [$F_{(5,42)}$=12.091, **p<0.001 vs. rest of the groups, ††p<0.01 vs. control, control-HFD, APP/PS1 and APP/PS1-HFD]; 0.5 mm [$F_{(5,44)}$=13.24, **p<0.001 vs. rest of the groups, ††p<0.01 vs. control, control-HFD, APP/PS1 and APP/PS1-HFD]; -0.5 mm [$F_{(5,45)}$=13.20, **p<0.001 vs. rest of the groups, ††p<0.01 vs. control, control-HFD, APP/PS1 and APP/PS1-HFD]; -1.5 mm [$F_{(5,44)}$=18.78, **p<0.001 vs. rest of the groups, ††p<0.01 vs. control, control-HFD, APP/PS1 and APP/PS1-HFD]; -2.5 mm $F_{(5,44)}$=1.87, **p<0.001 vs. rest of the groups, ††p<0.01 vs. control, control-HFD, APP/PS1 and APP/PS1-HFD]; -3.5 mm [$F_{(5,43)}$=16.772, **p<0.001 vs. rest of the groups, ††p<0.01 vs. control, control-HFD, APP/PS1 and APP/PS1-HFD]. **C)** Representative image of cortical thickness measured in all groups under study. Cortical thickness is indicated by green lines and measured. Scale bar=250 μm.

Figure 2. Caspase activation is increased and proportion of neurons are reduced in APP/PS1xdb/db mice. A) Activation of cortical caspases 3 and 7 was significantly increased in db/db mice and this effect was exacerbated in APP/PS1xdb/db mice. Differences were detected by one-way ANOVA followed by Tuckey b test [$F_{(5,26)}$=11.86, **p<0.01 vs. rest of the groups, ††p<0.01 vs. control, control-HFD, APP/PS1 and APP/PS1-HFD]. **B)** A slight reduction in the NeuN+/DAPI ratio was observed far from SP in APP/PS1-HFD mice. Higher reductions were observed in db/db mice and this effect was worsened in APP/PS1xdb/db mice when compared with the rest of the groups [$F_{(3,1120)}$=41.41, **p<0.01 vs. rest of the groups, ††p<0.01 vs. control, control-HFD, APP/PS1 and APP/PS1-HFD, ‡‡p<0.01 vs. Control and control-HFD. In the proximity of SP reduced NeuN+/DAPI ratios were observed when compared to SP free areas and this effect was worsened in APP/PS1xdb/db mice [$F_{(2,371)}$=7.53, **p<0.01 vs. rest of the groups]. **C)** Representative images of NeuN+/DAPI ratios in all groups under study (NeuN-red, DAPI-blue, thioflavin S-green). Scale bar=25 μm.

Figure 3. Amyloid pathology is altered in APP/PS1-HFD and APP/PS1xdb/db mice. A) Aβ deposits were increased after HFD treatment, whereas dense core SP were reduced in APP/PS1xdb/db mice measured by TS staining (anti-Aβ immunostaining [$F_{(2,105)}$=20.70, **p<0.01 vs. rest of the groups, ††p<0.01 vs. Control] and TS staining ([$F_{(2,104)}$=15.30, **p<0.01 vs. rest of the groups, ††p<0.01 vs. Control]). **B)** Illustrative example of anti-Aβ (red) and TS (green) staining in SP bearing groups. Scale bar=125 μm. **C)** Insoluble Aβ levels corroborated these observations and insoluble Aβ40 levels were increased in APP/PS1-HFD mice, whereas a significant reduction was observed in APP/PS1xdb/db mice [$F_{(2,28)}$=13.70, **p<0.01 vs. rest of the groups, ††p<0.01 vs. Control] although no statistical differences were detected for insoluble Aβ42 levels [$F_{(2,30)}$=2.85, p=0.074]. Measurement of soluble Aβ levels revealed an overall increase of both Aβ40 and Aβ4 in APP/PS1-HFD mice that reached statistical significance in case of APP/PS1xdb/db animals ([$F_{(2,28)}$=10.28, **p<0.001 vs. APP/PS1 and APP/PS1-HFD groups] and [$F_{(2,29)}$=8.25, ††p<0.001 vs. APP/PS1] respectively). Differences were detected by one-way ANOVA for independent samples followed by Tukey b or Tamhane tests as required.

Figure 4. Neurite curvature was increased in APP/PS1-HFD mice and this effect was worsened in APP/PS1xdb/db mice. A) Curvature ratios were slightly increased in APP/PS1 in SP free areas when compared with control groups. Also, neurite curvature was significantly increased in db/db mice, and this effect was worsened in APP/PS1xdb/db mice when we compared SP free areas in all groups under study. Data are representative of 5 mice and differences were detected by one-way ANOVA followed by Tamhane test [$F_{(5,4404)}$=101.206, **p<0.01 vs. rest of the groups, ††p<0.01 vs. control, control-HFD, APP/PS1 and APP/PS1-HFD, ‡‡p<0.01 vs. control and control-HFD]. Curvature ratios were significantly increased in the proximity of SP, and this effect was worsened in APP/PS1xd/db mice when compared with APP/PS1 and APP/PS1-HFD mice [$F_{(2,283)}$=3.22, *p<0.01 vs. APP/PS1 and APP/PS1-HFD]. **B)** Illustrative images of axon curvature stained with SMI-312R antibody (red) and SP stained with TS (green). Representative axons are marked in purple. Increased curvature ratios were also observed in db/db mice when compared with control mice. SP-bearing mice also show a higher

neurite curvature ratio and this effect is increased in APP/PS1xdb/db mice. Scale bar= 20 µm. **C)** Curvature ratios were reduced with increased distances to SP, when plotted in 10 µm subsets, in plaque-bearing groups. We observed a distance X group effect, and further assessment of individual subsets revealed that APP/PS1xdb/db mice presented a significantly higher curvature ratio than APP/PS1 and APP/PS1-HFD mice, whereas prediabetic APP/PS1 mice were similar to other groups. Differences were detected by one-way ANOVA for independent samples, follwed by Tukey b or Tamhane as required: <10 µm [$F_{(2,284)}$=3.170, *p=0.043 vs. APP/PS1 and APP/PS1-HFD], 10-20 µm [$F_{(2,621)}$=13.868, **p<0.01 vs. APP/PS1 and APP/PS1-HFD], 20-30 µm [$F_{(2,614)}$=16.154, **p<0.01 vs. APP/PS1 and APP/PS1-HFD, ††p<0.01 vs. APP/PS1], 30-40 µm [$F_{(2,532)}$=8.707, **p<0.01 vs. APP/PS1 and APP/PS1-HFD], >40 µm [$F_{(2,2134)}$=148.493, **p<0.01 vs. APP/PS1 and APP/PS1-HFD].

Figure 5. Array tomography analysis revealed reduction in synaptic density in diabetic mice. A) Synaptic density was determined by array tomography of PSD-95 labelled cortical slices. In the absence of plaques, synaptic density was reduced in db/db mice as well as in APP/PS1 and APP/PS1-HFD mice (SP-free areas) when compared to controls. Differences were detected by one-way ANOVA for independent samples followed by Tamhane test [$F_{(5,1148)}$=14.75, **p<0.01 vs. rest of the groups, ‡‡p<0.01 vs. control and control-HFD]. An overall reduction in synaptic density was observed in SP-bearing mice and this effect was more severe in case of APP/PS1xdb/db mice. Differences were detected by one-way ANOVA for independent samples followed by Tamhane test [$F_{(2,146)}$=8,76, **p<0.01 vs. APP/PS1 and APP/PS1-HFD]. **B)** A "halo" effect on synaptic density was observed in SP-bearing mice, when 10 µm steps from SP were used. An overall reduction of synaptic density was observed in APP/PS1xdb/db mice when compared with APP/PS1 mice. Differences were detected by one-way ANOVA followed by Tukey b or Tamhane tests; <10 µm from SP [$F_{(2,143)}$=12.9, ††p<0.001 vs. APP/PS1], 10-20 µm [$F_{(2,143)}$=10.42, **p<0.01 vs. APP/PS1 and APP/PS1-HFD groups], 20-30 µm [$F_{(2,142)}$=6.62, ††p<=0.004 vs. APP/PS1], 30-40 µm [$F_{(2,130)}$=3.26, †p=0.04 vs. APP/PS1], >40 µm [$F_{(2,486)}$=9.88, ††p<0.01 vs. APP/PS1]. **B)** Representative image of synaptic staining with PSD95 antibody for excitatory synapses (red), SP stained with 6E10 antibody (green) and

nuclear staining with DAPI (blue). A reduction in red puncta can be observed in db/db mice. An "halo" effect can be observed around SP, especially in APP/PS1xdb/db mice. Scale bar=10 μm.

References

[1] Serrano-Pozo A, Frosch MP, Masliah E, Hyman BT: Neuropathological alterations in Alzheimer disease. *Cold Spring Harb Perspect Med* 2011, **1**:a006189

[2] Beeri MS, Haroutunian V, Schmeidler J, Sano M, Fam P, Kavanaugh A, Barr AM, Honer WG, Katsel P: Synaptic protein deficits are associated with dementia irrespective of extreme old age. *Neurobiol Aging* 2012, **33**:1125 e1121-1128

[3] Robinson JL, Molina-Porcel L, Corrada MM, Raible K, Lee EB, Lee VM, Kawas CH, Trojanowski JQ: Perforant path synaptic loss correlates with cognitive impairment and Alzheimer's disease in the oldest-old. *Brain* 2014, **137**:2578-2587

[4] Luchsinger JA, Tang MX, Shea S, Mayeux R: Hyperinsulinemia and risk of Alzheimer disease. *Neurology* 2004, **63**:1187-1192

[5] Rundek T, Gardener H, Xu Q, Goldberg RB, Wright CB, Boden-Albala B, Disla N, Paik MC, Elkind MS, Sacco RL: Insulin resistance and risk of ischemic stroke among nondiabetic individuals from the northern Manhattan study. *Arch Neurol* 2010, **67**:1195-1200

[6] Schrijvers EM, Witteman JC, Sijbrands EJ, Hofman A, Koudstaal PJ, Breteler MM: Insulin metabolism and the risk of Alzheimer disease: the Rotterdam Study. *Neurology* 2010, **75**:1982-1987

[7] Arvanitakis Z, Wilson RS, Bienias JL, Evans DA, Bennett DA: Diabetes mellitus and risk of Alzheimer disease and decline in cognitive function. *Arch Neurol* 2004, **61**:661-666

[8] Cheng G, Huang C, Deng H, Wang H: Diabetes as a risk factor for dementia and mild cognitive impairment: a meta-analysis of longitudinal studies. *Intern Med J* 2012, **42**:484-491

[9] Luchsinger JA, Reitz C, Patel B, Tang MX, Manly JJ, Mayeux R: Relation of diabetes to mild cognitive impairment. *Arch Neurol* 2007, **64**:570-575

[10] Craft S: The role of metabolic disorders in Alzheimer disease and vascular dementia: two roads converged. *Arch Neurol* 2009, **66**:300-305

[11] Zhao WQ, De Felice FG, Fernandez S, Chen H, Lambert MP, Quon MJ, Krafft GA, Klein WL: Amyloid beta oligomers induce impairment of neuronal insulin receptors. *Faseb J* 2008, **22**:246-260

[12] Hyman BT: Amyloid-dependent and amyloid-independent stages of Alzheimer disease. *Arch Neurol* 2011, **68**:1062-1064

[13] Eckman EA, Eckman CB: Abeta-degrading enzymes: modulators of Alzheimer's disease pathogenesis and targets for therapeutic intervention. *Biochem Soc Trans* 2005, **33**:1101-1105

[14] Farris W, Mansourian S, Chang Y, Lindsley L, Eckman EA, Frosch MP, Eckman CB, Tanzi RE, Selkoe DJ, Guenette S: Insulin-degrading enzyme regulates the levels of insulin, amyloid beta-protein, and the beta-amyloid precursor protein intracellular domain in vivo. *Proc Natl Acad Sci U S A* 2003, **100**:4162-4167

[15] Bosco D, Fava A, Plastino M, Montalcini T, Pujia A: Possible implications of insulin resistance and glucose metabolism in Alzheimer's disease pathogenesis. *J Cell Mol Med* 2011, **15**:1807-1821

[16] Garcia-Alloza M: Streptozotocin as a tool to induce central pathology and cognitive impairment in rodents. *Streptozotocin: Uses, Mechanism of Action and Side Effects Editor: Gauthier, E L Nova Science Publishers, Inc Hauppauge, NY*
2014,

[17] De Felice FG, Ferreira ST: Inflammation, defective insulin signaling, and mitochondrial dysfunction as common molecular denominators connecting type 2 diabetes to Alzheimer disease. *Diabetes* 2014, **63**:2262-2272

[18] Jolivalt CG, Lee CA, Beiswenger KK, Smith JL, Orlov M, Torrance MA, Masliah E: Defective insulin signaling pathway and increased glycogen synthase kinase-3 activity in the brain of diabetic mice: parallels with Alzheimer's disease and correction by insulin. *J Neurosci Res* 2008, **86**:3265-3274
[19] Ramos-Rodriguez JJ, Jimenez-Palomares M, Murillo-Carretero MI, Infante-Garcia C, Berrocoso E, Hernandez-Pacho F, Lechuga-Sancho AM, Cozar-Castellano I, Garcia-Alloza M: Central vascular disease and exacerbated pathology in a mixed model of type 2 diabetes and Alzheimer's disease. *Psychoneuroendocrinology* 2015, **62**:69-79
[20] Ramos-Rodriguez JJ, Ortiz-Barajas O, Gamero-Carrasco C, de la Rosa PR, Infante-Garcia C, Zopeque-Garcia N, Lechuga-Sancho AM, Garcia-Alloza M: Prediabetes-induced vascular alterations exacerbate central pathology in APPswe/PS1dE9 mice. *Psychoneuroendocrinology* 2014, **48C**:123-135
[21] Takeda S, Sato N, Uchio-Yamada K, Sawada K, Kunieda T, Takeuchi D, Kurinami H, Shinohara M, Rakugi H, Morishita R: Diabetes-accelerated memory dysfunction via cerebrovascular inflammation and Abeta deposition in an Alzheimer mouse model with diabetes. *Proc Natl Acad Sci U S A* 2010, **107**:7036-7041
[22] Jankowsky JL, Slunt HH, Gonzales V, Jenkins NA, Copeland NG, Borchelt DR: APP processing and amyloid deposition in mice haplo-insufficient for presenilin 1. *Neurobiol Aging* 2004, **25**:885-892
[23] Garcia-Alloza M, Robbins EM, Zhang-Nunes SX, Purcell SM, Betensky RA, Raju S, Prada C, Greenberg SM, Bacskai BJ, Frosch MP: Characterization of amyloid deposition in the APPswe/PS1dE9 mouse model of Alzheimer disease. *Neurobiol Dis* 2006, **24**:516-524
[24] Ramos-Rodriguez JJ, Ortiz O, Jimenez-Palomares M, Kay KR, Berrocoso E, Murillo-Carretero MI, Perdomo G, Spires-Jones T, Cozar-Castellano I, Lechuga-Sancho AM, Garcia-Alloza M: Differential central pathology and cognitive impairment in pre-diabetic and diabetic mice. *Psychoneuroendocrinology* 2013,
[25] Koffie RM, Meyer-Luehmann M, Hashimoto T, Adams KW, Mielke ML, Garcia-Alloza M, Micheva KD, Smith SJ, Kim ML, Lee VM, Hyman BT, Spires-Jones TL: Oligomeric amyloid beta associates with postsynaptic densities and correlates with excitatory synapse loss near senile plaques. *Proc Natl Acad Sci U S A* 2009, **106**:4012-4017
[26] Franklin KBJ, Paxinos G: The Mouse Brain in Stereotaxic Coordinates. *Academic Press United States* 1997,
[27] Ramos-Rodriguez JJ, Pacheco-Herrero M, Thyssen D, Murillo-Carretero MI, Berrocoso E, Spires-Jones TL, Bacskai BJ, Garcia-Alloza M: Rapid beta-amyloid deposition and cognitive impairment after cholinergic denervation in APP/PS1 mice. *J Neuropathol Exp Neurol* 2013, **72**:272-285
[28] Ramos-Rodriguez JJ, Molina-Gil S, Rey-Brea R, Berrocoso E, Garcia-Alloza M: Specific Serotonergic Denervation Affects tau Pathology and Cognition without Altering Senile Plaques Deposition in APP/PS1 Mice. *PLoS One* 2013, **8**:e79947
[29] Ramos-Rodriguez JJ, Infante-Garcia C, Galindo-Gonzalez L, Garcia-Molina Y, Lechuga-Sancho A, Garcia-Alloza M: Increased Spontaneous Central Bleeding and Cognition Impairment in APP/PS1 Mice with Poorly Controlled Diabetes Mellitus. *Mol Neurobiol* 2015,
[30] Garcia-Alloza M, Borrelli LA, Rozkalne A, Hyman BT, Bacskai BJ: Curcumin labels amyloid pathology in vivo, disrupts existing plaques, and partially restores distorted neurites in an Alzheimer mouse model. *J Neurochem* 2007, **102**:1095-1104
[31] Ramos-Rodriguez JJ, Molina-Gil S, Ortiz-Barajas O, Jimenez-Palomares M, Perdomo G, Cozar-Castellano I, Lechuga-Sancho AM, Garcia-Alloza M: Central

proliferation and neurogenesis is impaired in type 2 diabetes and prediabetes animal models. *PLoS One* 2014, **9**:e89229
[32] Maesako M, Uemura K, Iwata A, Kubota M, Watanabe K, Uemura M, Noda Y, Asada-Utsugi M, Kihara T, Takahashi R, Shimohama S, Kinoshita A: Continuation of exercise is necessary to inhibit high fat diet-induced beta-amyloid deposition and memory deficit in amyloid precursor protein transgenic mice. *PLoS One* 2013, **8**:e72796
[33] D'Amore JD, Kajdasz ST, McLellan ME, Bacskai BJ, Stern EA, Hyman BT: In vivo multiphoton imaging of a transgenic mouse model of Alzheimer disease reveals marked thioflavine-S-associated alterations in neurite trajectories. *J Neuropathol Exp Neurol* 2003, **62**:137-145
[34] Garcia-Alloza M, Dodwell SA, Meyer-Luehmann M, Hyman BT, Bacskai BJ: Plaque-derived oxidative stress mediates distorted neurite trajectories in the Alzheimer mouse model. *J Neuropathol Exp Neurol* 2006, **65**:1082-1089
[35] Meyer-Luehmann M, Spires-Jones TL, Prada C, Garcia-Alloza M, de Calignon A, Rozkalne A, Koenigsknecht-Talboo J, Holtzman DM, Bacskai BJ, Hyman BT: Rapid appearance and local toxicity of amyloid-beta plaques in a mouse model of Alzheimer's disease. *Nature* 2008, **451**:720-724
[36] Jimenez-Palomares M, Ramos-Rodriguez JJ, Lopez-Acosta JF, Pacheco-Herrero M, Lechuga-Sancho AM, Perdomo G, Garcia-Alloza M, Cozar-Castellano I: Increased Abeta production prompts the onset of glucose intolerance and insulin resistance. *Am J Physiol Endocrinol Metab* 2012, **11**:1373-1380
[37] Perez SE, Dar S, Ikonomovic MD, DeKosky ST, Mufson EJ: Cholinergic forebrain degeneration in the APPswe/PS1DeltaE9 transgenic mouse. *Neurobiol Dis* 2007, **28**:3-15
[38] den Heijer T, Vermeer SE, van Dijk EJ, Prins ND, Koudstaal PJ, Hofman A, Breteler MM: Type 2 diabetes and atrophy of medial temporal lobe structures on brain MRI. *Diabetologia* 2003, **46**:1604-1610
[39] Moran C, Phan TG, Chen J, Blizzard L, Beare R, Venn A, Munch G, Wood AG, Forbes J, Greenaway TM, Pearson S, Srikanth V: Brain Atrophy in Type 2 Diabetes: Regional distribution and influence on cognition. *Diabetes Care* 2013,
[40] Hummel KP, Dickie MM, Coleman DL: Diabetes, a new mutation in the mouse. *Science* 1966, **153**:1127-1128
[41] Farr SA, Banks WA, Morley JE: Effects of leptin on memory processing. *Peptides* 2006, **27**:1420-1425
[42] Li XL, Aou S, Oomura Y, Hori N, Fukunaga K, Hori T: Impairment of long-term potentiation and spatial memory in leptin receptor-deficient rodents. *Neuroscience* 2002, **113**:607-615
[43] Kim B, Feldman EL: Insulin resistance in the nervous system. *Trends Endocrinol Metab* 2012, **23**:133-141
[44] Stern EA, Bacskai BJ, Hickey GA, Attenello FJ, Lombardo JA, Hyman BT: Cortical synaptic integration in vivo is disrupted by amyloid-beta plaques. *J Neurosci* 2004, **24**:4535-4540
[45] Shankar GM, Li S, Mehta TH, Garcia-Munoz A, Shepardson NE, Smith I, Brett FM, Farrell MA, Rowan MJ, Lemere CA, Regan CM, Walsh DM, Sabatini BL, Selkoe DJ: Amyloid-beta protein dimers isolated directly from Alzheimer's brains impair synaptic plasticity and memory. *Nat Med* 2008, **14**:837-842
[46] Infante-Garcia C, Ramos-Rodriguez JJ, Galindo-Gonzalez L, Garcia-Alloza M: Long-term central pathology and cognitive impairment are exacerbated in a mixed model of Alzheimer's disease and type 2 diabetes. *Psychoneuroendocrinology* 2016, **65**:15-25

[47] Walsh DM, Selkoe DJ: Deciphering the molecular basis of memory failure in Alzheimer's disease. *Neuron* 2004, **44**:181-193

Figure

Click here to download Figure Figure 1 new.tif

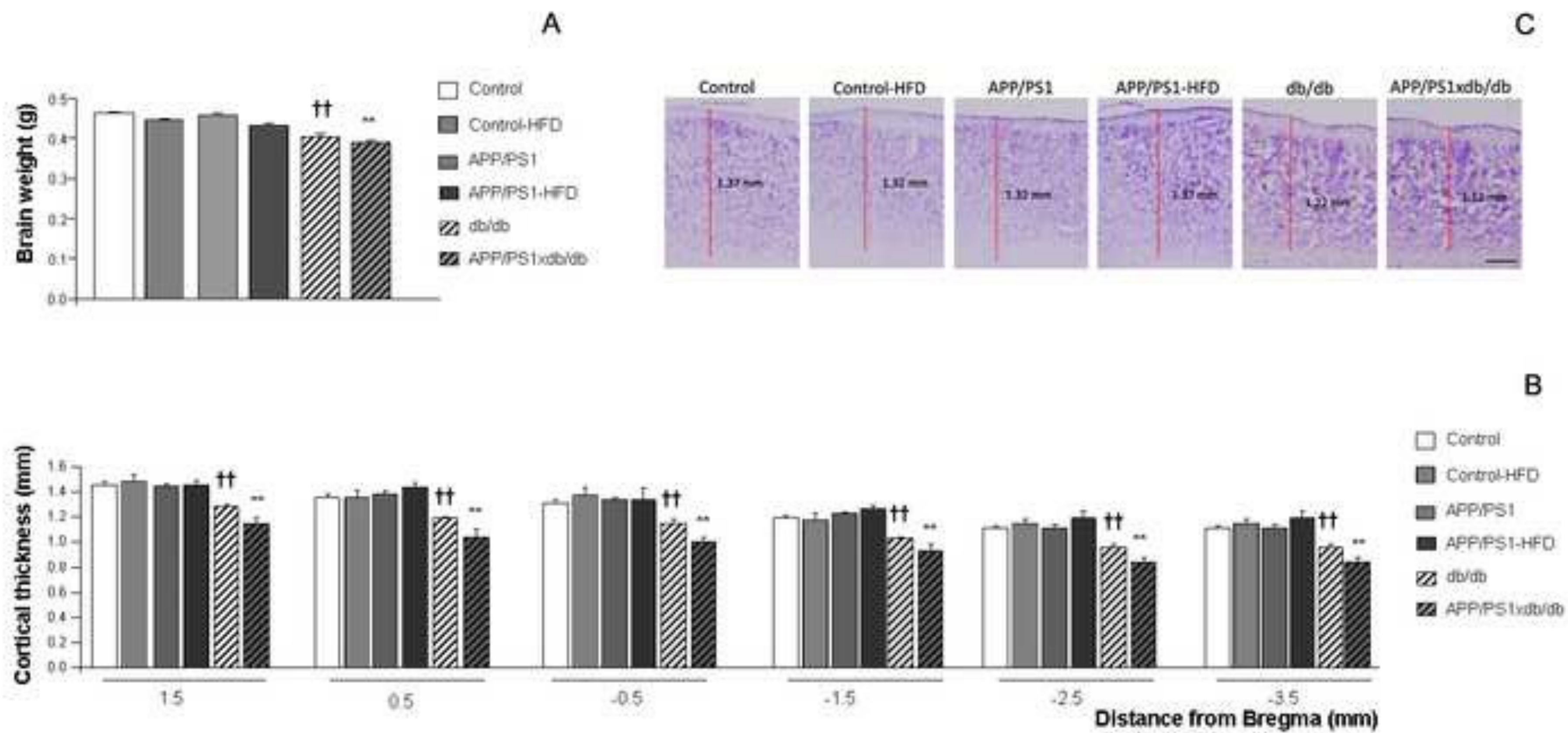

Click here to download Figure Figure 2.tif

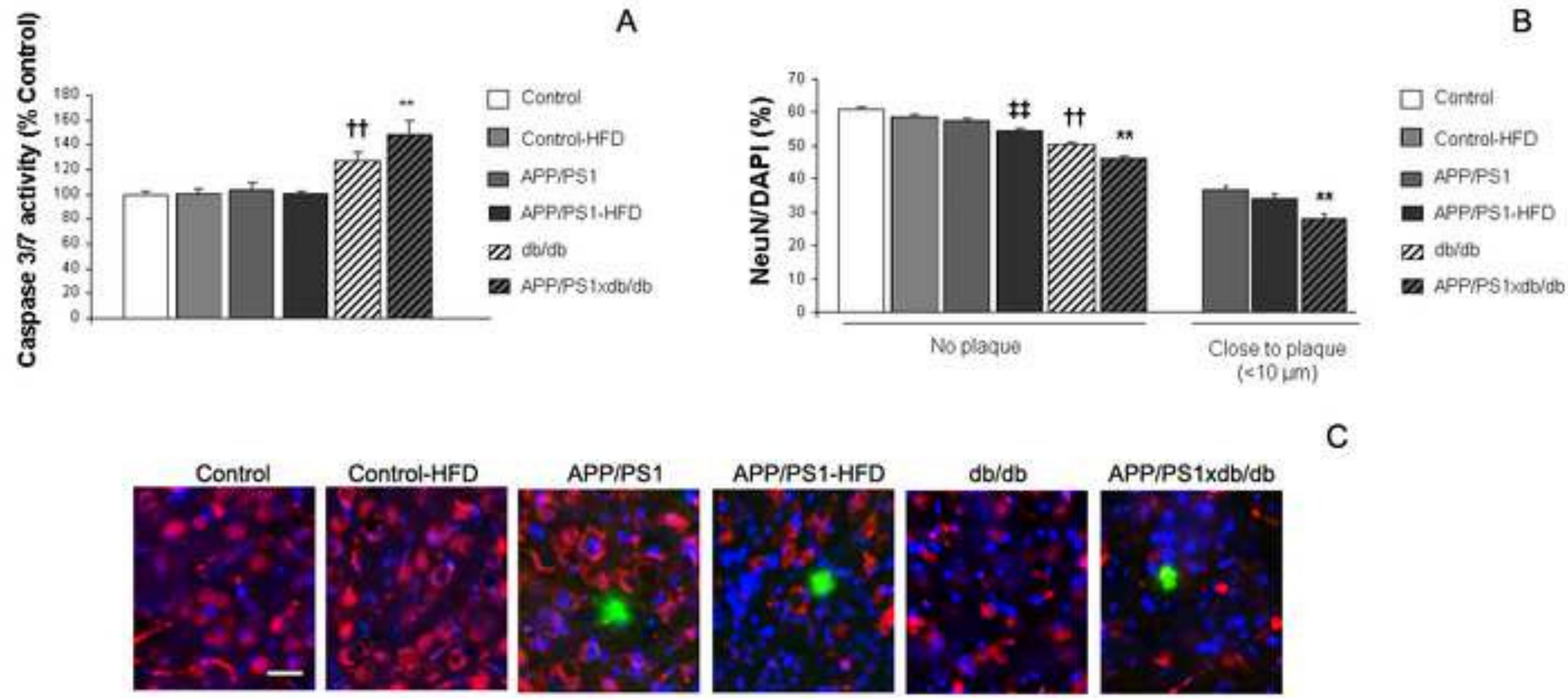

Figure

Click here to download Figure Figure 3 new.tif

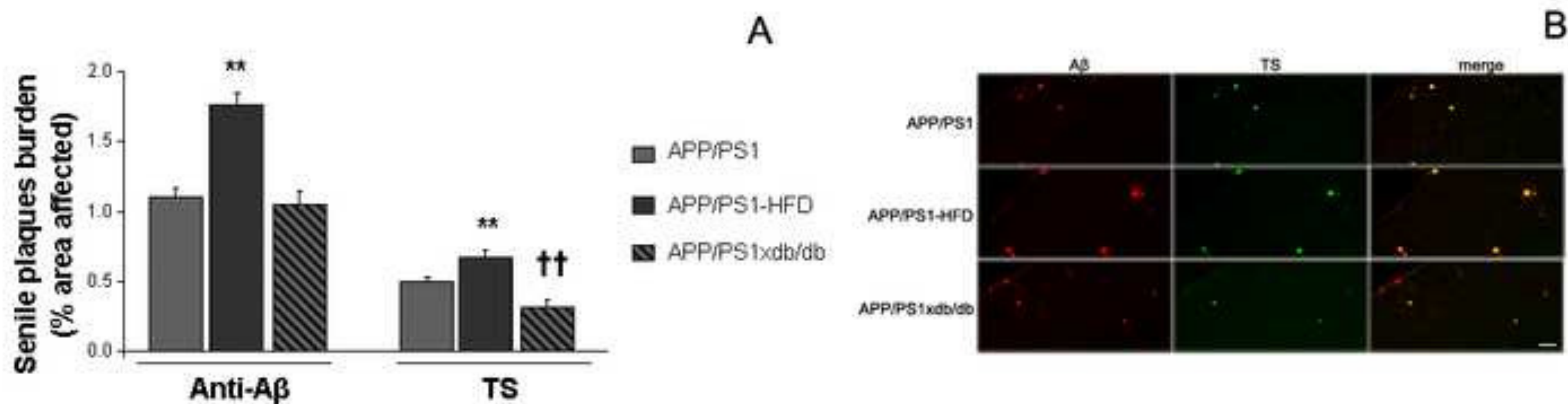

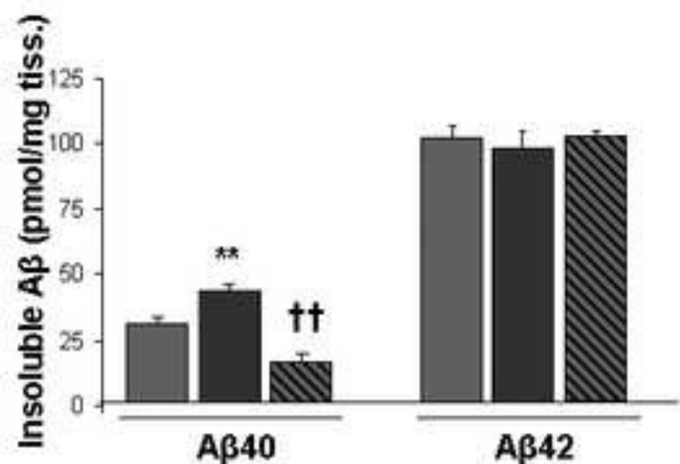

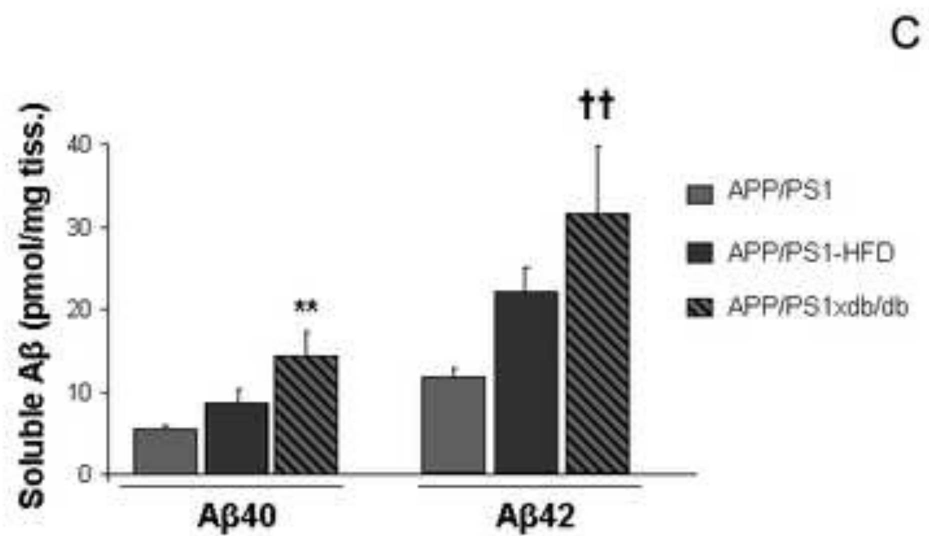

Figure

Click here to download Figure Figure 4 new.tif

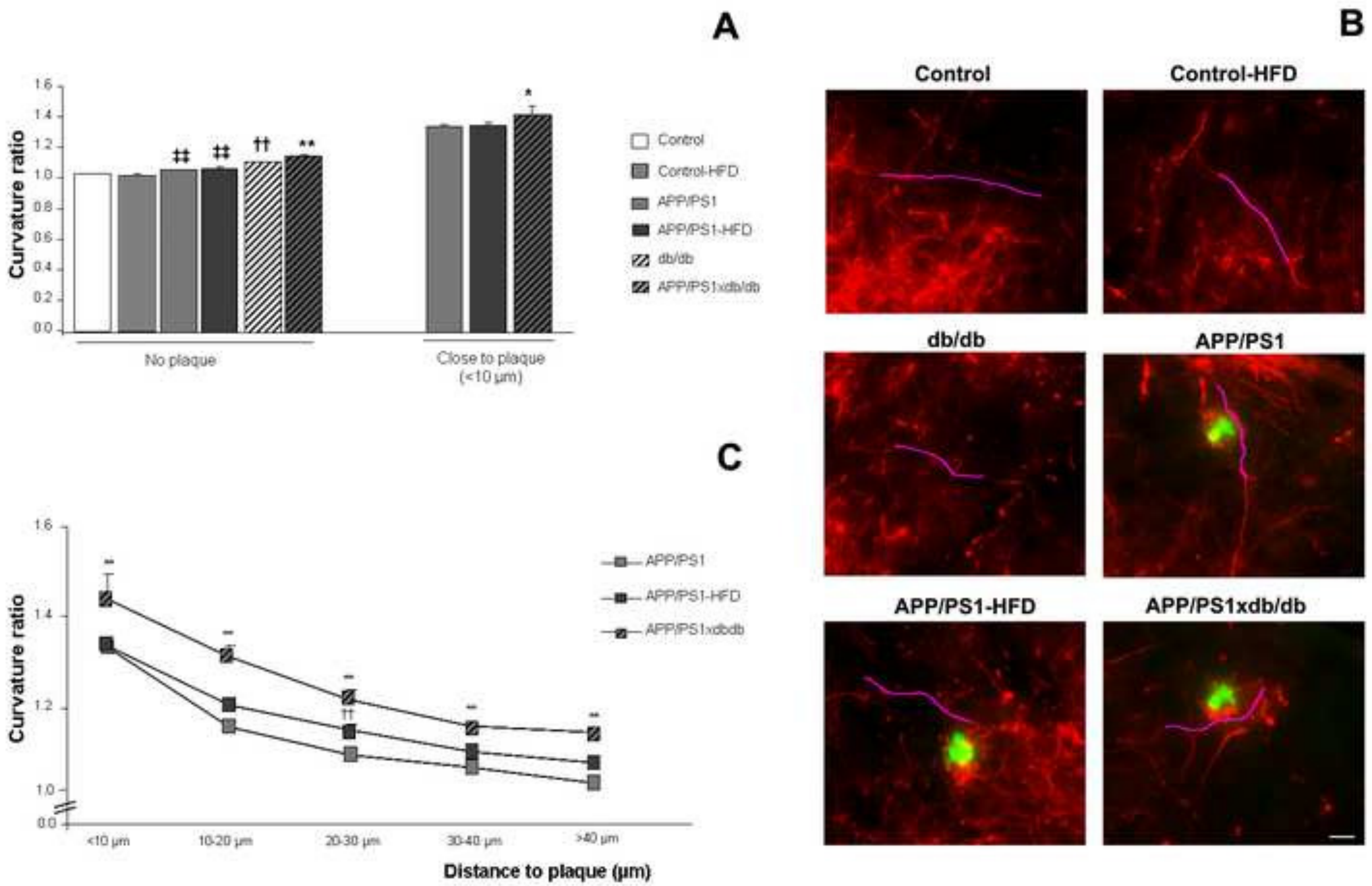

Click here to download Figure Figure 5 new.tif